Peer-reviewed version available at *Antioxidants* **2020**, *9*, 775; doi:10.3390/antiox9090775

Article

In silico identification and biological evaluation of antioxidant food components endowed with IX and XII *h*CA inhibition

Giosuè Costa [1,2#], Annalisa Maruca [1,2#], Roberta Rocca [2,3], Francesca Alessandra Ambrosio [1], Emanuela Berrino[4], Fabrizio Carta [4], Francesco Mesiti [1,2], Alessandro Salatino [3], Delia Lanzillotta [3], Francesco Trapasso [3], Anna Artese [1,2], Stefano Alcaro [1,2*] and Claudiu T. Supuran [4]

[1] Dipartimento di Scienze della Salute, Università "Magna Græcia" di Catanzaro, Campus "S. Venuta", Viale Europa, 88100, Catanzaro, Italy; gcosta@unicz.it (G.C.); maruca@unicz.it (A.M.); ambrosio@unicz.it (F.A.A); francesco.mesiti@studenti.unicz.it (F.M); artese@unicz.it (A.A.); alcaro@unicz.it (S.A)

[2] Net4Science Academic Spin-Off, Università "Magna Græcia" di Catanzaro, Campus "S. Venuta", Viale Europa, 88100, Catanzaro, Italy; rocca@unicz.it (R.R.)

[3] Dipartimento di Medicina Sperimentale e Clinica, Università "Magna Græcia" di Catanzaro, Campus "S. Venuta", Viale Europa, 88100, Catanzaro, Italy; salatino@unicz.it (A.S); delialanzillotta@unicz.it (D.L.); trapasso@unicz.it (F.T)

[4] Dipartimento NEUROFARBA, Sezione di Scienze Farmaceutiche, Università degli Studi di Firenze, Sesto Fiorentino, Florence, Italy; emanuela.berrino@unifi.it (E.B.); fabrizio.carta@unifi.it (F.C); claudiu.supuran@unifi.it (C.T.S.)

* Correspondence: alcaro@unicz.it; Tel.+39 0961 3694198 (S. A.)

#These authors contributed equally.

Abstract: The tumour-associated isoenzymes *h*CA IX and *h*CA XII catalyze the hydration of carbon dioxide to bicarbonate and protons. These isoforms are highly overexpressed in many types of cancer, where they contribute for the acidification of the tumor environment promoting the tumor cell invasion and metastasis. In this work, in order to identify novel dual *h*CA IX and XII inhibitors, virtual screening techniques and biological assays were combined. A structure-based virtual screening towards *h*CA IX and XII was performed using a database of approximately 26000 natural compounds. The best shared *hits* were submitted to a thermodynamic analysis and 3 promising best *hits* were identified and evaluated in terms of their *h*CA IX and XII inhibitor activity. *In vitro* biological assays were in line with the theoretical studies and revealed that Syringin, Lithospermic acid, and (-)- Dehydrodiconiferyl alcohol behave as good *h*CA IX and *h*CA XII dual inhibitors.

Keywords: *h*CA IX and XII; dual inhibitors; molecular modeling studies; *in vitro* assays.

1. Introduction

The Carbonic Anhydrases (CAs, EC 4.2.1.1) are metalloenzyme that reversibly catalyze the hydration of carbon dioxide (CO_2) to bicarbonate (HCO_3^-) and proton (H^+) ions. These enzymes are grouped into eight distinct and not related genetic families (α, β, γ, δ, ζ, η θ-, and ι-CAs) and are a typical example of biological convergent evolution directed toward the catalysis of essential biochemical processes[1-3]. The human CAs (*h*CAs) belong to the α-class and exist in 15 different isoforms, which differ for tissue distribution, subcellular localization, and catalytic activity. In

Peer-reviewed version available at Antioxidants 2020, 9, 775; doi:10.3390/antiox9090775

particular, *h*CA I-III, *h*CA VII, and *h*CA XIII are cytosolic isozymes, *h*CA VA and VB are located in the mitochondria, and *h*CA IV, *h*CA IX, *h*CAXII, and *h*CA XIV are membrane-bound isozymes[4]. These enzymes are distributed in human tissues and organs, where they are involved in critical physiological process, including pH regulation, electrolyte secretion, respiration, bone resorption among other[5]. Therefore, abnormal levels and/or activities of these enzymes usually are associated with several diseases, e.g. glaucoma, neurological disorder, osteoporosis, and metabolic disorders[6].

Recently, two specific *h*CA isoforms, namely *h*CA IX and *h*CA XII gained great attention[7]. They usually are refereed as the "tumor associate isoenzymes" in consideration of the specific localization and activity within hypoxic tumor tissues. In detail, *h*CA IX is ectopically induced and highly overexpressed in many solid tumors, including brain, breast, bladder, pancreas, and T-cell lymphomas[8]. Furthermore, it was observed that *h*CA IX is closely overexpressed in response to hypoxia in cancer cells, whereas *h*CA XII isoform is also upregulated in many tumor types, however its activity and expression are also profuse in normal tissues[9, 10]. Several evidences demonstrated that *h*CA IX and *h*CA XII inhibitors affect the pH of the tumor microenvironment reducing tumor cell survival and proliferation[11, 12]. Due to their implication on tumorigenicity and cancer metastasis, *h*CA IX and *h*CA XII isoforms have been widely investigated, and several *h*CAs inhibitors were developed as promising anticancer agents. Encouraging *in vitro* and *in vivo* studies have shown that the inhibition of *h*CA IX and *h*CA XII decreases growth, proliferation and metastatic potential of different cancers[13, 14]. In this respect, the sulfonamide (and their structural related bioisosteres, sulfamates and sulfamides) and the coumarins/thiocoumarins-based *h*CA IX/*h*CA XII inhibitors showed promising results[15-18]. In parallel, natural occurring compounds, especially phenol derivatives figured out significant antioxidant activities and remarkable *h*CAs inhibitory capacity[19-21]. Guaiacol, a plant isolated compound, and several catechol derivatives effectively inhibited *h*CA IX and *h*CA XII with K_i at low micromolar range[21].

Nowadays, cancer is ranked as the second cause of death worldwide, therefore the development of new anticancer therapies is an urgent need[22, 23]. Furthermore, the design of new molecules with a multi-targeting profile could be a useful approach to face oncogenesis and cancer progression[24-27]. Moreover, in the development of *h*CAs inhibitors, a special attention should be given to their selective profile. In fact, several drugs interaction and side effects have linked to non-selective *h*CAs inhibition, thus a selective profile over the appropriate isoforms is mandatory[7, 28]. Under this light, selective *h*CA IX and *h*CA XII inhibitors could be considered as potential anti-cancer drugs[18].

In the drug discovery process, the application of computational methods has demonstrated to be important for the identification of new *hit* compounds. The *in silico* studies are able to speed the identification of bioactive compounds, thus reducing cost and time of research associated activities[29]. In particular, structure-based virtual screening (SBVS) consists in a computational tool helpful to identify novel bioactive ligands towards a selective target(s), exploiting the three-dimensional (3D) structures of the biological target, either protein or nucleic acid[30-36]. Many natural products and/or food constituent molecules have been considered in the treatment of serious diseases, including cancer[37, 38]. FooDB[39] is the most comprehensive online database providing information about food constituent molecules, their chemical structures, and concentrations in various foods. Within this framework and in the continuous research of potent and selective *h*CA IX and *h*CA XII inhibitors, we performed a SBVS using a database of natural occurring compounds. FooDB database was used to build up a chemical library of natural occurring compounds virtually screened towards several *h*CAs. The most promising compounds, selected based on their theoretical binding energy, were further submitted to *in vitro* assays to point out new promising *h*CA IX and *h*CA XII inhibitors. The experimental results confirmed the computational predictions, providing the rationale behind the ligands biological activity and selectivity.

2. Materials and Methods

2.1 Molecular modeling studies

Starting from the three dimensional structure of the human carbonic anhydrase IX in complex with 5-(1-naphthalen-1-yl-1,2,3-triazol-4-yl)thiophene-2-sulfonamide and the crystal structure of the human carbonic anhydrase isozyme XII with 2,3,5,6-tetrafluoro-4-(propylthio)benzenesulfonamide, deposited in the Protein Data Bank (PDB) with the PDB codes 5FL4[40] and 5MSA[41], respectively, our molecular modeling simulations were carried out.

In order to evaluate the reliability of our molecular recognition approach, we performed redocking calculations by using Glide Standard Protocol (SP) algorithm, that was able to reproduce the experimentally determined binding modes. In fact, we obtained Root Mean Square Deviation (RMSD) values, calculated between the best docking pose and the ligand co-crystallized into the *h*CA IX and XII catalytic binding site, equal to 0.545 Å and 1.059 Å for the *h*CA IX and *h*CA XII, respectively.

The receptor structures were prepared by means of the Protein Preparation Wizard tool implemented in Maestro, using OLPS_2005 as force field. Residual crystallographic buffer components were removed, missing side chains were built using the Prime module, hydrogen atoms were added, side chains protonation states at pH 7.4 were assigned and water molecules were deleted[42, 43].

For the Virtual Screening (VS) studies, the FooDB database, containing 26680 compounds, was used[39]. The library was prepared by means of LigPrep tool[44], hydrogens were added, salts were removed, ionization states were calculated using Ionizer at pH 7.4 and then all the compounds were submitted to energy minimization, using OPLS_2005 as force field, thus obtaining 25584 compounds. Glide v. 6.7 SP algorithm was used to perform VS[45] and 10 poses for ligands were generated.

In order to select the scored compounds according to their Glide-score (G-score) value, we performed molecular docking studies of already approved and investigational *h*CA isoforms IX (**2**-**5**) and XII (**1**-**5**) inhibitors (Figure S1), such as Acetozolamide, Zonisamide and Ellagic acid, and we obtained a consensus value to be applied as filter (Tables S1-S2). Starting from the best shared *hits* resulted from VS simulations, a post-docking energy minimization was applied using the eMBrAcE tool developed by Schrödinger (MacroModel v10.8)[46, 47] and the binding energies (ΔE) between ligands and receptors were calculated. Each complex was subjected to energy minimization in implicit solvent, using the conjugate gradient protocol and OPLS_2005 as force field. The average ΔE values of the already approved and investigational *h*CA isoforms IX and XII inhibitors, respectively, were used to further filter the obtained *hits*.

Finally, the shared compounds between both *h*CA isoforms IX and *h*CA XII were investigated by visual inspection. Then, based on their commercial availability, we purchased 3 best *hits* which were submitted to *in vitro* assays.

2.2 Carbonic Anhydrase Inhibition Assay

An Applied Photophysics stopped-flow instrument has been used for assaying the CA-catalyzed CO_2 hydration activity[48]. Phenol red (at a concentration of 0.2 mM) has been used as an indicator, working at the absorbance maximum of 557 nm, with 20 mM Hepes (pH 7.5) as a buffer, and 20 mM Na_2SO_4 (for maintaining the ionic strength constant), following the initial rates of the CA-catalyzed CO_2 hydration reaction for a period of 10−100 s. The CO_2 concentrations ranged from 1.7 to 17 mM for the determination of the kinetic parameters and inhibition constants. For each inhibitor, at least six traces of the initial 5−10% of the reaction have been used for determining the initial velocity. The uncatalyzed rates were determined in the same manner and subtracted from the total observed rates. Stock solutions of the inhibitor (0.1 mM) were prepared in distilled deionized water, and dilutions up to 0.01 nM were done thereafter with the assay buffer. The inhibitor and enzyme solutions were preincubated together for 30 min at r.t. prior to the assay, in order to allow for the formation of the E−I complex. The inhibition constants were obtained by nonlinear least-squares methods using PRISM 3 and the Cheng−Prusoff equation, as reported earlier, and represent the mean from at least three different determinations. All CA isoforms were recombinant ones obtained in-house as reported earlier[49, 50].

2.3 Inhibition Growth Assay

The human colorectal cancer cells Caco-2 were cultured in DMEM medium (Sigma Aldrich, St. Louis, Missouri, USA) supplemented with 10% fetal bovine serum (FBS) (Sigma Aldrich, St. Louis, Missouri, USA), 1% Penicillin/Streptomycin (Sigma Aldrich, St. Louis, Missouri, USA). Cells were grown in a 5% CO2 incubator at 37° C. Cell viability was assessed through a MMT assay: 104 cells/well were seeded in a 96-well plate and, two hours later, treated with 6, 12 and 14 (the latter dissolved in DMSO) at 10 μM concentration. After 24, 48 and 72 hours, 20 μL of MTT detection reagent, 3-(4,5-dimethylthiazol-2-yl)-2,5-diphenyl tetrazolium (Sigma Aldrich, St. Louis, Missouri, USA) (5 mg/mL), was added, and the plate was incubated for two more hours[51]. Culture medium was removed and 200 μL of isopropanol (0,04 M HCl) were added to dissolve formazan crystals. Absorbance was measured at 560 nm by Victor 3 reader.

3. Results

3.1. Structure-Based Virtual Screening (SBVS)

In this study, by using a SBVS approach, about 26 thousand food components were screened against both *h*CA IX and XII isoforms. Starting from the active set (Tables S1 and S2), we applied a *cut-off* to filter the obtained *hits*, thus considering for *h*CA IX and XII the average Glide SP scores of -5.11 kcal/mol and -5.38 kcal/mol, respectively.

This first filter led to select 7364 and 6552 *hits* from *h*CA IX and XII, respectively. Afterwards, we calculated the binding energies of the 4430 shared *hits* in complex with both receptors with the aim to investigate their thermodynamic profile. In order to select the best promising *hits* with a potential dual activity, we applied the same protocol also for the active set (**1**-**5**) (Tables S1 and S2). Therefore, their average ΔE values, equal to -21.92 kcal/mol and -28.19 kcal/mol for *h*CA IX and XII, respectively, were used as *cut-off*, globally leading to 988 *hits*, characterized by a good theoretical dual activity.

Finally, after a careful visual inspection analysis of the best poses, 9 *hits* (**6–14**) were selected (Table S3). Structurally, all the selected *hits* showed hydroxides, phenols, and carboxylic acids as recurring chemical scaffolds, confirming the essential role of these moieties in the molecular recognition of both *h*CA IX and XII isoforms (Figure S1). Unfortunately, the evaluation of their commercial availability revealed that only 3 compounds (**6**, **12**, and **14**) could be purchased and submitted to biological assays. Among them, compound **12** was found to have a good inhibitory activity on *h*CA XII[52], thus we included it in the biological screening also on the IX isoform, to further validate our protocol aimed at discovering new dual inhibitors for both *h*CAs involved in tumors pathogenesis.

All the VS steps are summarized in Figure 1.

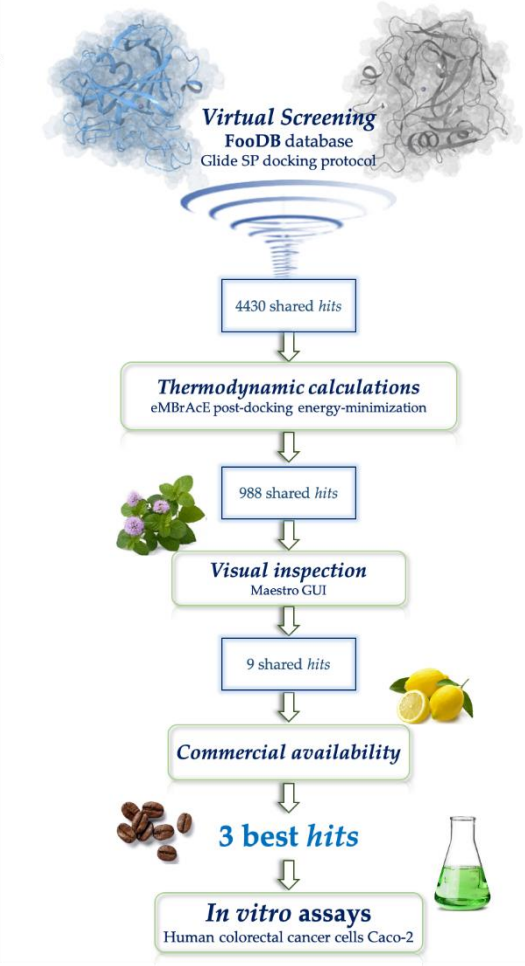

Figure1. Representation of the SBSV workflow.

3.2. Carbonic Anhydrase Inhibition Assay

The selected compounds **6**, **12** and **14** were evaluated *in vitro* for their inhibition potencies against the most relevant *h*CAs such as the cytosolic and widely expressed *h*CAs I, II and the tumor associated *h*CAs IX and XII. The obtained data reported below in Table 1 were all compared to the standard *h*CA inhibitor Acetazolamide (**AAZ**).

Table 1. Inhibition data of *h*CA I, II, IX, and XII with **6**, **12**, **14** and the standard sulfonamide inhibitor Acetazolamide (**AAZ**) by the Stopped-Flow CO_2 Hydrase Assay.

	***h*CA I**	***h*CA II**	***h*CA IX**	***h*CA XII**
6	>100	>100	2.59	0.096
12	>100[52]	>100[52]	0.31	0.0048[52]
14	>100	>100	0.32	0.092
AAZ	0.250	0.012	0.026	0.0057

*Mean from three different assays by a stopped-flow technique (errors were in the range of ±5−10% of the reported values).

Peer-reviewed version available at Antioxidants 2020, 9, 775; doi:10.3390/antiox9090775

Overall, the compounds considered resulted ineffective inhibitors against the widely expressed *h*CAs I and II with K_Is >100 μM. Interesting results were obtained for the remaining isoforms:

i) As for the **14** the data reported in Table 1 clearly showed the tumor associated *h*CA XII isoform was 3.5-fold more potently inhibited when compared to the *h*CA IX (K_Is of 0.092 and 0.32 μM respectively) with a selectivity index (SI; K_I *h*CA IX/ K_I *h*CA XII) of 3.5;

ii) The same kinetic profile was also recovered for the **6** although enhanced enzymatic SIs were observed. The tumor associated *h*CA XII resulted inhibited 27.0-fold more potently when compared to the IX (K_Is of 0.096 and 2.59 μM respectively);

iii) **12** was already investigated as potential inhibitor *h*CA on the widely expressed *h*CAs I, II and on the tumor associated IX and XII from some authors of this manuscript and the data reported in Table 1 were in good agreement[52]. It is worth considering that an impressive *h*CA XII selective inhibition was obtained from such a substance, thus being the most potent and selective against such a tumor associated isoform (K_Is of 0.31 and 0.0048 μM for the *h*CA IX and XII respectively).

The kinetic data here reported clearly showed **6**, **12** and **14** being effective inhibitors of the tumor associated *h*CA IX and XII and in particular, the latter was preferentially inhibited with K_I values in the low micromolar range. Among the substances tested the **12** was particularly potent inhibitor of the *h*CA XII having a K_I value close to the reference drug of the sulfonamide type AAZ (K_Is of 0.0048 and 0.0057 μM respectively).

3.3. Docking pose and thermodynamic analysis of the best hits

By evaluating their docking best poses, all 3 *hits* were well recognized into the catalytic binding site of both *h*CA IX and XII, as shown in Figure 2. By using the Maestro graphical interface[53] contact analysis, we observed all compounds able to strongly interact with the binding pocket residues of both tumors associated *h*CAs by means of hydrogen bond (H-bond), salt bridges, electrostatic and cation interactions. Moreover, the better affinity of all 3 *hits* towards *h*CA XII could be rationalized by the higher number of good contacts and H-bonds with respect to the *h*CA IX isoform (Table 2).

Table 2. Hydrogen bonds (HB), salt bridges (SB), good contacts (GC), stacking (S) and cation (C) interactions established by the 3 best *hits* with the *h*CA IX and XII receptor targets.

	***h*CA IX**					***h*CA XII**				
Hit	**HB**	**SB**	**GC**	**S**	**C**	**HB**	**SB**	**GC**	**S**	**C**
6	3	0	179	0	0	4	0	222	0	0
12	8	0	167	1	0	7	2	291	0	1
14	3	0	224	0	0	4	0	222	0	0

Regarding **12** best pose, we found its two carboxyl groups involved in two salt bridge interactions with the side chain of Lys69 and Lys3 in *h*CA XII binding pocket (Figure 2e). The same

Peer-reviewed version available at *Antioxidants* **2020**, *9*, 775; doi:10.3390/antiox9090775

groups engaged different H-bonds with Lys3, Trp4, Lys69 and Gln89, thus further stabilizing the complex. Moreover, the pyrocatechol ring established a cation interaction and an H-bond with the side chain of Lys3 and Asn94, respectively, while the pyrocatechol linked to dihydrofuran interacted with Thr198 by means of two H-bonds. Conversely, as shown in Figure 2 (b), the pyrocatechol linked to the dihydrofuran moiety established four H-bonds with the side chains of Asn66 and Arg64, meanwhile the other pyrocathecol ring was involved in a stacking interaction and one H-bond with the side chain of His94 and Tyr11, respectively. With respect to *h*CA XII, we highlighted that **12** formed an H-bond network among its two carboxyl groups and the residues Trp9, Hie68, and Gln92.

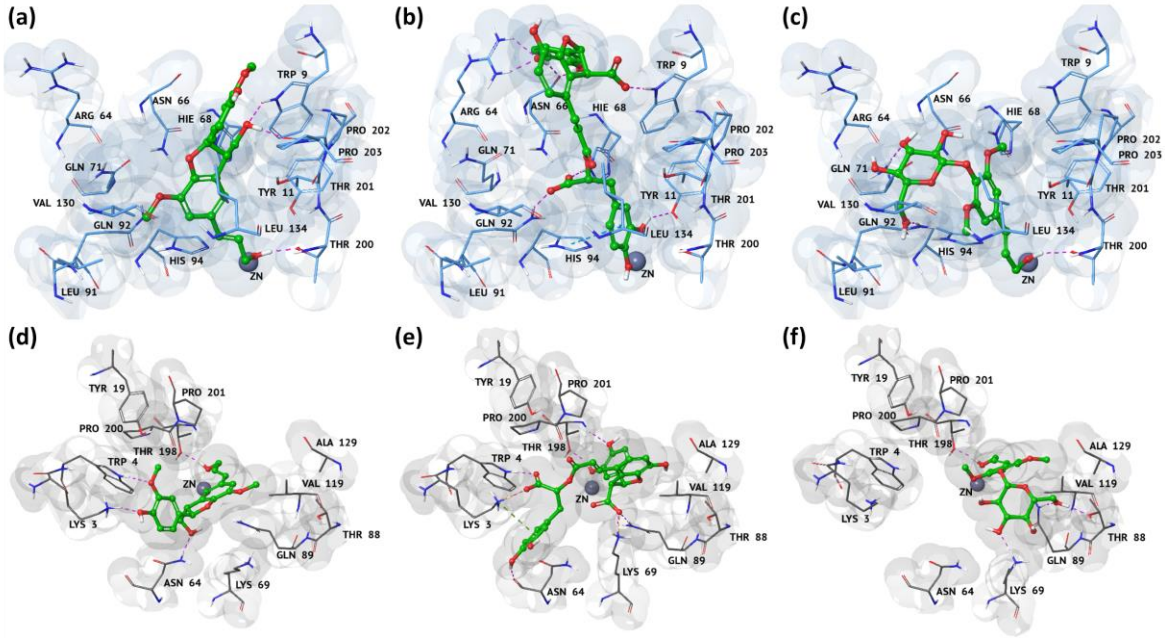

Figure 2. 3D representations of the binding mode of (**a-d**) **6**, (**b-e**) **12** and (**c-f**) **14** best *hits* against *h*CA IX and XII binding pockets, respectively. The ligands are depicted as green carbon sticks, while *h*CA IX and XII are shown as blue and gray transparent cartoon, respectively. The zinc cation is represented as violet sphere and the enzyme residues, involved in crucial contacts with the compounds, are reported as blue and gray carbon sticks, respectively for *h*CA IX and XII isoforms. Hydrogen bonds, salt bridges, cation and stacking interactions are reported, respectively, as dashed pink, orange, green and light-blue lines. These binding modes derived from the molecular mechanics energy minimization performed by means of the eMBrAcE tool.

Regarding compound **6,** the alcohol groups were involved in the most important interactions into both isoforms pockets (Figure 2 a-d). Specifically, in *h*CA IX the allyl alcohol of **6** engaged an H-bond with the side chain of Thr200, while the primary alcohol interacted with the side chain of Trp9 and the backbone of Pro202 (Figure 2a). Conversely, in *h*CA XII the same groups were involved in two H-bonds with Thr198 and Asn64. The two additional H-bonds, found between the phenolic moiety of **6** and the side chains of Lys3 and Trp9, further increased its affinity towards the XII isoform, as confirmed by the biological assays (Figure 2d). Finally, as reported in Table 2, **6** was able to establish several productive interactions with both the *h*CA isoforms.

By analyzing the binding pose of **14**, we observed that the sugar moiety and the allylic alcohol were implicated in pivotal interactions. In detail, we found that the sugar moiety established two H-bonds with *h*CA IX Gln71 and Gln92, meanwhile the same portion was able to form three H-bonds with Lys69, Thr88 and Val119 residues of *h*CA XII. Finally, the allylic alcohol was involved in an H-bond with Thr200 and Thr198 of the IX and XII isoforms, respectively.

The detailed evaluation of **6**, **12** and **14** thermodynamic profile against *h*CA IX and XII isoforms showed the eMBrAcE protocol able to well predict their good dual activity, as confirmed by the

biological results. By investigating the single contributions of the ΔE energy components, we observed the electrostatic term as the driven force in the binding process for both targets (Table 3).

Table 3. eMBrAcE ΔE values and their single contributions, expressed as electrostatic, van der Waals and solvation components (ΔE_{Elec}, ΔE_{vdW} and ΔE_{Solv}), calculated for the 3 best *hits* complexed with *h*CA IX and XII receptors. All thermodynamic values are reported in kcal/mol.

		***h*CA IX**				***h*CA XII**			
Hit	**FooDB ID**	**ΔE**	**ΔE_{Elec}**	**ΔE_{vdW}**	**ΔE_{Solv}**	**ΔE**	**ΔE_{Elec}**	**ΔE_{vdW}**	**ΔE_{Solv}**
6	FDB021188	-37.89	-71.80	-17.28	46.18	-43.75	-110.89	-25.64	81.26
12	FDB006174	-23.42	-59.74	-12.72	37.79	-31.83	-227.57	-28.01	206.77
14	FDB011657	-31.22	-36.62	-22.44	26.06	-43.81	-105.69	-22.33	73.05

3.4. Cell viability assay

In order to investigate the biological effects of **6**, **12** and **14**, we carried out a MTT assay on Caco-2 cancer cells. Cell viability was assessed at different time points (24, 48 and 72 hours) after treatment. No significant effects were assessed twenty-four hours after treatment (data not shown).
Interestingly, the most significant effects were observed seventy-two hours after treatment with all used compounds, ranging from nearly 70% of cell viability (**6**) to approximatively 50% of cell viability (**12** and **14**) (Figure 3).
Taken together, these results suggest a potential anticancer activity of the analysed compounds, thus encouraging their further development.

Peer-reviewed version available at *Antioxidants* **2020**, *9*, 775; doi:10.3390/antiox9090775

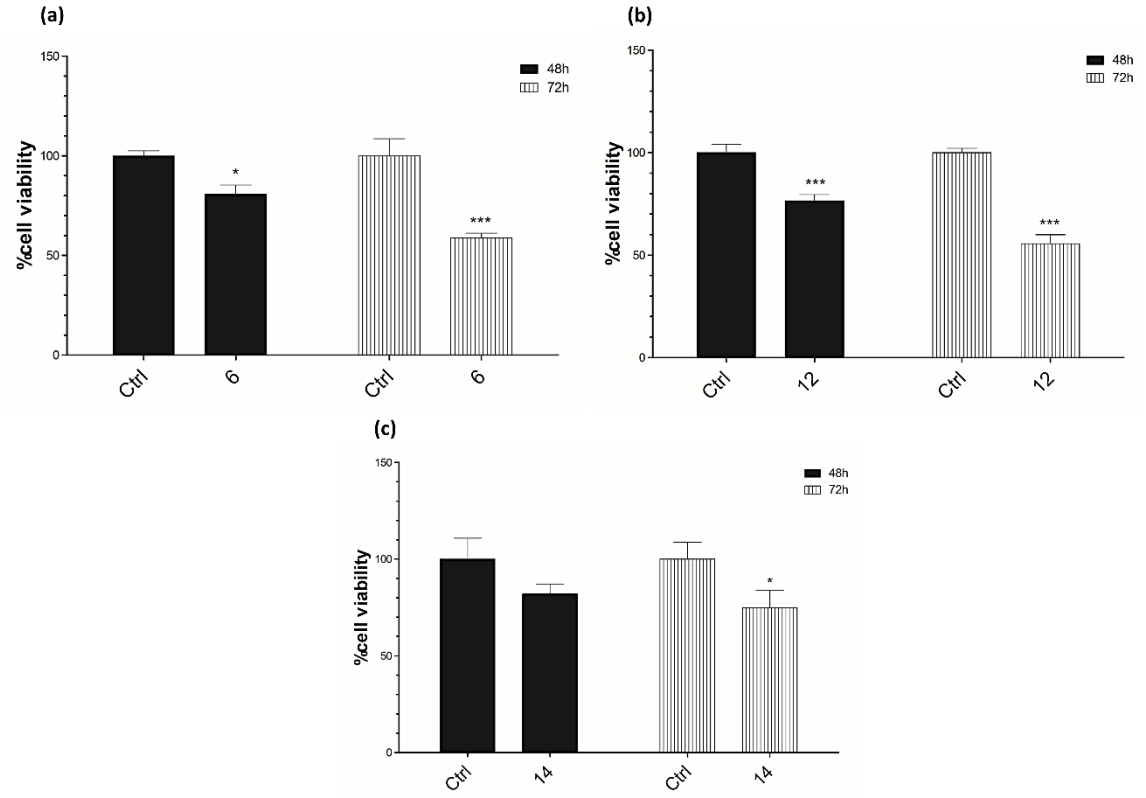

Figure 3. Effects of 6, 12 and 14 on Caco-2 cell viability.
1x103 cells were plated, in triplicate, in 96-well plates and treated with compounds at the concentration of 10 μM for 48 and 72 hours; cells treated with DMSO were used as control. Cell viability was measured performing a MTT assay and expressed as a percentage of control, analyzed by ANOVA (*p<0.05; **p<0.005; ***p<0.0005), each column represents the mean ± SD of three different wells.

4. Discussion

The molecular modeling studies put on evidence the presence of the phenolic moiety in all best *hits*. Such a scaffold is known to be incorporated in several antioxidant compounds and, more recently, was found to have a key role in inhibiting *h*CA I and II [54].

6, **12** and **14** are food constituents, thus confirming the strong importance of natural components as source of lead and bioactive compounds, able to affect several biological processes in our organism. In fact, many studies in literature have demonstrated that natural products with anti-inflammatory, antimicrobial and antioxidant activity could be useful for multifactorial diseases[37, 38].

Among the 3 *hits*, compound **6** is known as (-)-Dehydrodiconiferyl Alcohol, and belongs to the class of organic compounds known as 2-arylbenzofuran flavonoids. It has been detected, but not quantified, in coffee and coffee products and green vegetables. In literature, it was found to exert anti-*Helicobacter pylori*[55], anti-adipogenic,[56] and antioxidant effects[57]. Recently, Lee *et al.* reported that (-)-Dehydrodiconiferyl Alcohol suppresses the p38 MAPK and NF-κB signalling pathways in RAW 264.7 cells and acts as an estrogen receptor agonist [58]. Moreover, it exerts anti-inflammatory activity by regulating key molecules involved in inflammation and oxidative stress, such as pro-inflammatory cytokines (TNF-α, IL-6 and IL-1β) and mediators (iNOS, COX-2 and ROS)[59].

As compound **6**, the Lithospermic acid **12** is a member of the class of 2-arylbenzofuran flavonoids and it is also known as lithospermate. Our approach highlighted it as the most interesting dual inhibitor of both *h*CAs, in line with a previous work related to its *h*CA XII[52] proven activity. It can be found in common thyme and peppermint, which makes lithospermic acid a potential biomarker for the consumption of these food products, and it showed a good and well-known antioxidant activity[60, 61].

Finally, **14** is Syringin, also known as eleutheroside b or β-terpineol. It belongs to phenolic glycosides, that are organic compounds containing a phenolic structure attached to a glycosyl moiety. Syringin was first isolated from the bark of lilac (*Syringa vulgaris*) by Meillet in 1841. Moreover, it can be found in caraway, fennel, and lemon, which makes syringin a potential biomarker for the consumption of these food products. Several pharmacological actions of syringin include plasma glucose reduction, anti-oxidation, anti-cancer activity, antidepressant effect and immunomodulation[62, 63].

In vitro results demonstrated that all the 3 *hits* are able to inhibit both *h*CA IX and XII isoforms in the micromolar range, although with a preference towards the XII target, thus confirming their potential anticancer activity.

5. Conclusions

In this work, *in silico* and experimental techniques were combined to identify natural bioactive compounds present in food, such as coffee, green vegetables, common thyme, peppermint, caraway, fennel, and lemon, and endowed with inhibition properties against both *h*CA IX and XII isoforms. All the best *hits* are characterized by a phenol moiety, which has recently aroused considerable interest because of its potential beneficial biochemical and antioxidant effects on human health. Polyphenols, commonly referred to as antioxidants, may prevent different diseases associated with oxidative stress, such as cancers, cardiovascular diseases, inflammation and others. Thus, the identification and validation of targets combination associated with a desired clinical effect, by avoiding the off-target effect, have obtained increasing attention.

Our approach allowed us to identify (-)- Dehydrodiconiferyl alcohol, Lithospermic acid and Syringin as good *h*CA IX and *h*CA XII dual inhibitors with a potential anticancer activity, thus encouraging their further development. Specifically, Lithospermic acid and Syringin, associated to K_I values in the low micromolar range, showed a better cytotoxic effect seventy-two hours after treatment than (-)- Dehydrodiconiferyl alcohol.

Supplementary Materials: The following are available online at www.mdpi.com/xxx/s1, Figure S1: 2D chemical structures of the already approved inhibitor of both *h*CA isoforms, Table S1: 2D chemical structures, G-score and ΔE values for each already approved inhibitor of the *h*CA isoform XII, Table S2: 2D chemical structures, G-score and ΔE values for each already approved inhibitor of the *h*CA isoform IX, Table S3: Name and FooDB ID of the 9 best dual *hits*, obtained by Structure Based Virtual Screening, and their G-score and ΔE values related to both *h*CA isoforms, Figure S2.: 2D chemical structures of the best 9 selected *hits*.

Author Contributions: Conceptualization, G.C. and A.A.; methodology, F.A.A., E.B. and A.S.; validation, A.M., R.R., F.A.A.; formal analysis, A.M., R.R., D.L.; investigation, G.C., A.S. and F.C.; resources, S.A.; data curation, A.M., F.C. and D.L.; writing—original draft preparation, A.M., R.R., F.M., F.A.A. and F.C. ; writing—review and editing, G.C., A.A., S.A. and F.T.; visualization, F.M.; supervision, S.A., C.T.S. and F.T.; project administration, G.C., F.C. and F.T.; funding acquisition, S.A., C.T.S. and F.T. All authors have read and agreed to the published version of the manuscript.", please turn to the CRediT taxonomy for the term explanation. Authorship must be limited to those who have contributed substantially to the work reported.

Funding: This research was funded by PRIN 2017 research project "Novel anticancer agents endowed with multi-targeting mechanism of action", grant number 201744BN5T. A.M. was supported by MIUR research project "NUTRAMED PON 03PE000_78_2".

Acknowledgments: The authors acknowledge Mu.Ta.Lig. COST Action CA15135.

Conflicts of Interest: "The authors declare no conflict of interest."

References

1. Supuran, C. T., How many carbonic anhydrase inhibition mechanisms exist? *J. Enzyme Inhib. Med. Chem.* **2016,** 31, 345-360.

2. Mboge, M. Y.; McKenna, R.; Frost, S. C., Advances in Anti-Cancer Drug Development Targeting Carbonic Anhydrase IX and XII. *Top Anticancer Res.* **2015,** 5, 3-42.
3. Supuran, C. T., Exploring the multiple binding modes of inhibitors to carbonic anhydrases for novel drug discovery. *Expert Opin. Drug. Discov.* **2020,** 15, 671-686.
4. Supuran, C. T., Carbonic anhydrases--an overview. *Curr. Pharm. Des.* **2008,** 14, 603-614.
5. Supuran, C. T., Advances in structure-based drug discovery of carbonic anhydrase inhibitors. *Expert Opin. Drug Discov.* **2017,** 12, 61-88.
6. Supuran, C. T.; Scozzafava, A., Carbonic anhydrase inhibitors and their therapeutic potential. *Expert Opin. Ther. Pat.* **2000,** 10, 575-600.
7. Monti, S. M.; Supuran, C. T.; De Simone, G., Anticancer carbonic anhydrase inhibitors: a patent review (2008 - 2013). *Expert Opin. Ther. Pat.* **2013,** 23, 737-749.
8. Mboge, M. Y.; Mahon, B. P.; McKenna, R.; Frost, S. C., Carbonic Anhydrases: Role in pH Control and Cancer. *Metabolites* **2018,** 8, 19.
9. Morris, J. C.; Chiche, J.; Grellier, C.; Lopez, M.; Bornaghi, L. F.; Maresca, A.; Supuran, C. T.; Pouyssegur, J.; Poulsen, S. A., Targeting hypoxic tumor cell viability with carbohydrate-based carbonic anhydrase IX and XII inhibitors. *J. Med. Chem.* **2011,** 54, 6905-6918.
10. Guler, O. O.; De Simone, G.; Supuran, C. T., Drug design studies of the novel antitumor targets carbonic anhydrase IX and XII. *Curr. Med. Chem.* **2010,** 17, 1516-1526.
11. Mahon, B. P.; Bhatt, A.; Socorro, L.; Driscoll, J. M.; Okoh, C.; Lomelino, C. L.; Mboge, M. Y.; Kurian, J. J.; Tu, C.; Agbandje-McKenna, M.; Frost, S. C.; McKenna, R., The Structure of Carbonic Anhydrase IX Is Adapted for Low-pH Catalysis. *Biochemistry* **2016,** 55, 4642-4653.
12. Li, Y.; Tu, C.; Wang, H.; Silverman, D. N.; Frost, S. C., Catalysis and pH control by membrane-associated carbonic anhydrase IX in MDA-MB-231 breast cancer cells. *J. Biol. Chem.* **2011,** 286, 15789-15796.
13. Pacchiano, F.; Carta, F.; McDonald, P. C.; Lou, Y.; Vullo, D.; Scozzafava, A.; Dedhar, S.; Supuran, C. T., Ureido-substituted benzenesulfonamides potently inhibit carbonic anhydrase IX and show antimetastatic activity in a model of breast cancer metastasis. *J. Med. Chem.* **2011,** 54, 1896-1902.
14. Yang, J. S.; Lin, C. W.; Chuang, C. Y.; Su, S. C.; Lin, S. H.; Yang, S. F., Carbonic anhydrase IX overexpression regulates the migration and progression in oral squamous cell carcinoma. *Tumour Biol.* **2015,** 36, 9517-9524.
15. Nocentini, A.; Ceruso, M.; Carta, F.; Supuran, C. T., 7-Aryl-triazolyl-substituted sulfocoumarins are potent, selective inhibitors of the tumor-associated carbonic anhydrase IX and XII. *J. Enzyme Inhib. Med. Chem.* **2016,** 31, 1226-1233.
16. Ozensoy, O.; Puccetti, L.; Fasolis, G.; Arslan, O.; Scozzafava, A.; Supuran, C. T., Carbonic anhydrase inhibitors: inhibition of the tumor-associated isozymes IX and XII with a library of aromatic and heteroaromatic sulfonamides. *Bioorg. Med. Chem. Lett.* **2005,** 15, 4862-4866.
17. Ibrahim, H. S.; Abou-Seri, S. M.; Tanc, M.; Elaasser, M. M.; Abdel-Aziz, H. A.; Supuran, C. T., Isatin-pyrazole benzenesulfonamide hybrids potently inhibit tumor-associated carbonic anhydrase isoforms IX and XII. *Eur. J. Med. Chem.* **2015,** 103, 583-593.
18. Supuran, C. T.; Winum, J. Y., Carbonic anhydrase IX inhibitors in cancer therapy: an update. *Future Med. Chem.* **2015,** 7, 1407-1414.
19. Innocenti, A.; Beyza Ozturk Sarikaya, S.; Gulcin, I.; Supuran, C. T., Carbonic anhydrase inhibitors. Inhibition of mammalian isoforms I-XIV with a series of natural product polyphenols and phenolic acids. *Bioorg. Med. Chem.* **2010,** 18, 2159-2164.
20. Ozturk Sarikaya, S. B.; Topal, F.; Senturk, M.; Gulcin, I.; Supuran, C. T., In vitro inhibition of alpha-carbonic anhydrase isozymes by some phenolic compounds. *Bioorg. Med. Chem. Lett.* **2011,** 21, 4259-4262.
21. Scozzafava, A.; Passaponti, M.; Supuran, C. T.; Gulcin, I., Carbonic anhydrase inhibitors: guaiacol and catechol derivatives effectively inhibit certain human carbonic anhydrase isoenzymes (hCA I, II, IX and XII). *J. Enzyme Inhib. Med. Chem.* **2015,** 30, 586-591.
22. Nagai, H.; Kim, Y. H., Cancer prevention from the perspective of global cancer burden patterns. *J. Thorac. Dis.* **2017,** 9, 448-451.
23. www.who.int.
24. Xie, L.; Bourne, P. E., Developing multi-target therapeutics to fine-tune the evolutionary dynamics of the cancer ecosystem. *Front. Pharmacol.* **2015,** 6, 209.
25. Raghavendra, N. M.; Pingili, D.; Kadasi, S.; Mettu, A.; Prasad, S., Dual or multi-targeting inhibitors: The next generation anticancer agents. *Eur. J. Med. Chem.* **2018,** 143, 1277-1300.
26. Cassetta, L.; Pollard, J. W., Targeting macrophages: therapeutic approaches in cancer. *Nat. Rev. Drug Discov.* **2018,** 17, 887-904.

27. Catalano, R.; Rocca, R.; Juli, G.; Costa, G.; Maruca, A.; Artese, A.; Caracciolo, D.; Tagliaferri, P.; Alcaro, S.; Tassone, P.; Amodio, N., A drug repurposing screening reveals a novel epigenetic activity of hydroxychloroquine. *Eur. J. Med. Chem.* **2019,** 183, 111715.
28. Alterio, V.; Di Fiore, A.; D'Ambrosio, K.; Supuran, C. T.; De Simone, G., Multiple binding modes of inhibitors to carbonic anhydrases: how to design specific drugs targeting 15 different isoforms? *Chem. Rev.* **2012,** 112, 4421-4468.
29. Gidaro, M. C.; Astorino, C.; Petzer, A.; Carradori, S.; Alcaro, F.; Costa, G.; Artese, A.; Rafele, G.; Russo, F. M.; Petzer, J. P.; Alcaro, S., Kaempferol as Selective Human MAO-A Inhibitor: Analytical Detection in Calabrian Red Wines, Biological and Molecular Modeling Studies. *J. Agric. Food Chem.* **2016,** 64, 1394-400.
30. Maruca, A.; Lanzillotta, D.; Rocca, R.; Lupia, A.; Costa, G.; Catalano, R.; Moraca, F.; Gaudio, E.; Ortuso, F.; Artese, A.; Trapasso, F.; Alcaro, S., Multi-Targeting Bioactive Compounds Extracted from Essential Oils as Kinase Inhibitors. *Molecules* **2020,** 25, 2174.
31. Rocca, R.; Moraca, F.; Costa, G.; Talarico, C.; Ortuso, F.; Da Ros, S.; Nicoletto, G.; Sissi, C.; Alcaro, S.; Artese, A., In Silico Identification of Piperidinyl-amine Derivatives as Novel Dual Binders of Oncogene c-myc/c-Kit G-quadruplexes. *ACS Med. Chem. Lett.* **2018,** 9, 848-853.
32. Costa, G.; Rocca, R.; Corona, A.; Grandi, N.; Moraca, F.; Romeo, I.; Talarico, C.; Gagliardi, M. G.; Ambrosio, F. A.; Ortuso, F.; Alcaro, S.; Distinto, S.; Maccioni, E.; Tramontano, E.; Artese, A., Novel natural non-nucleoside inhibitors of HIV-1 reverse transcriptase identified by shape- and structure-based virtual screening techniques. *Eur. J. Med. Chem.* **2019,** 161, 1-10.
33. Costa, G.; Carta, F.; Ambrosio, F. A.; Artese, A.; Ortuso, F.; Moraca, F.; Rocca, R.; Romeo, I.; Lupia, A.; Maruca, A.; Bagetta, D.; Catalano, R.; Vullo, D.; Alcaro, S.; Supuran, C. T., A computer-assisted discovery of novel potential anti-obesity compounds as selective carbonic anhydrase VA inhibitors. *Eur. J. Med. Chem.* **2019,** 181, 111565.
34. Rocca, R.; Moraca, F.; Costa, G.; Nadai, M.; Scalabrin, M.; Talarico, C.; Distinto, S.; Maccioni, E.; Ortuso, F.; Artese, A.; Alcaro, S.; Richter, S. N., Identification of G-quadruplex DNA/RNA binders: Structure-based virtual screening and biophysical characterization. *Biochim. Biophys. Acta Gen. Subj.* **2017,** 1861, 1329-1340.
35. Costa, G.; Rocca, R.; Moraca, F.; Talarico, C.; Romeo, I.; Ortuso, F.; Alcaro, S.; Artese, A., A Comparative Docking Strategy to Identify Polyphenolic Derivatives as Promising Antineoplastic Binders of G-quadruplex DNA c-myc and bcl-2 Sequences. *Mol. Inform.* **2016,** 35, 391-402.
36. Catalano, R.; Moraca, F.; Amato, J.; Cristofari, C.; Rigo, R.; Via, L. D.; Rocca, R.; Lupia, A.; Maruca, A.; Costa, G.; Catalanotti, B.; Artese, A.; Pagano, B.; Randazzo, A.; Sissi, C.; Novellino, E.; Alcaro, S., Targeting multiple G-quadruplex-forming DNA sequences: Design, biophysical and biological evaluations of indolo-naphthyridine scaffold derivatives. *Eur. J. Med. Chem.* **2019,** 182, 111627.
37. Bagetta, D.; Maruca, A.; Lupia, A.; Mesiti, F.; Catalano, R.; Romeo, I.; Moraca, F.; Ambrosio, F. A.; Costa, G.; Artese, A.; Ortuso, F.; Alcaro, S.; Rocca, R., Mediterranean products as promising source of multi-target agents in the treatment of metabolic syndrome. *Eur. J. Med. Chem.* **2020,** 186, 111903.
38. Maruca, A.; Catalano, R.; Bagetta, D.; Mesiti, F.; Ambrosio, F. A.; Romeo, I.; Moraca, F.; Rocca, R.; Ortuso, F.; Artese, A.; Costa, G.; Alcaro, S.; Lupia, A., The Mediterranean Diet as source of bioactive compounds with multi-targeting anti-cancer profile. *Eur. J. Med. Chem.* **2019,** 181, 111579.
39. foodb.ca.
40. Leitans, J.; Kazaks, A.; Balode, A.; Ivanova, J.; Zalubovskis, R.; Supuran, C. T.; Tars, K., Efficient Expression and Crystallization System of Cancer-Associated Carbonic Anhydrase Isoform IX. *J. Med. Chem.* **2015,** 58, 9004-9009.
41. Smirnov, A.; Manakova, E.; Grazulis, S., Crystal structure of human carbonic anhydrase isozyme XII with 2,3,5,6-Tetrafluoro-4-(propylthio)benzenesulfonamide. *10.2210/pdb5msa/pdb* **2018**.
42. Protein Preparation Wizard, Schrodinger, LLC, New York, NY. **2018**.
43. Prime, Schrodinger, LLC, New York, NY. **2018**.
44. LigPrep, Schrodinger, LLC, New York, NY. **2018**.
45. Glide, Schrödinger, LLC, New York, NY. **2018**.
46. Mohamadi, F.; Richards, N. G. J.; Guida, W. C.; Liskamp, R.; Lipton, M.; Caufield, C.; Chang, G.; Hendrickson, T.; Still, W. C., MacroModel—an integrated software system for modeling organic and bioorganic molecules using molecular mechanics. *J. Comput. Chem.* **1990,** 11, 440–467.
47. Schrödinger LLC, NY, USA. **2018**.
48. Khalifah, R. G., The carbon dioxide hydration activity of carbonic anhydrase. I. Stop-flow kinetic studies on the native human isoenzymes B and C. *J. Biol. Chem.* **1971,** 246, 2561-2573.

49. Berrino, E.; Angeli, A.; Zhdanov, D. D.; Kiryukhina, A. P.; Milaneschi, A.; De Luca, A.; Bozdag, M.; Carradori, S.; Selleri, S.; Bartolucci, G.; Peat, T. S.; Ferraroni, M.; Supuran, C. T.; Carta, F., Azidothymidine "Clicked" into 1,2,3-Triazoles: First Report on Carbonic Anhydrase-Telomerase Dual-Hybrid Inhibitors. *J. Med. Chem.* **2020,** 63, 7392–7409.
50. Angeli, A.; Carta, F.; Donnini, S.; Capperucci, A.; Ferraroni, M.; Tanini, D.; Supuran, C. T., Selenolesterase enzyme activity of carbonic anhydrases. *Chem. Commun. (Camb)* **2020,** 56, 4444-4447.
51. Barone, A.; Mendes, M.; Cabral, C.; Mare, R.; Paolino, D.; Vitorino, C., Hybrid Nanostructured Films for Topical Administration of Simvastatin as Coadjuvant Treatment of Melanoma. *J. Pharm. Sci.* **2019,** 108, 3396-3407.
52. Karioti, A.; Ceruso, M.; Carta, F.; Bilia, A. R.; Supuran, C. T., New natural product carbonic anhydrase inhibitors incorporating phenol moieties. *Bioorg. Med. Chem.* **2015,** 23, 7219-7225.
53. Maestro Graphics User Interface, Schrödinger LLC, New York, NY, USA. **2018**.
54. Riafrecha, L. E.; Bua, S.; Supuran, C. T.; Colinas, P. A., Synthesis and carbonic anhydrase inhibitory effects of new N-glycosylsulfonamides incorporating the phenol moiety. *Bioorg. Med. Chem. Lett.* **2016,** 26, 3892-3895.
55. Hu, K.; Jeong, J. H., A convenient synthesis of an anti-Helicobacter pylori agent, dehydrodiconiferyl alcohol. *Arch. Pharm. Res.* **2006,** 29, 563-565.
56. Lee, J.; Kim, D.; Choi, J.; Choi, H.; Ryu, J. H.; Jeong, J.; Park, E. J.; Kim, S. H.; Kim, S., Dehydrodiconiferyl alcohol isolated from Cucurbita moschata shows anti-adipogenic and anti-lipogenic effects in 3T3-L1 cells and primary mouse embryonic fibroblasts. *J. Biol. Chem.* **2012,** 287, 8839-8851.
57. Lee, J.; Kim, S., Upregulation of heme oxygenase-1 expression by dehydrodiconiferyl alcohol (DHCA) through the AMPK-Nrf2 dependent pathway. *Toxicol. Appl. Pharmacol.* **2014,** 281, 87-100.
58. Lee, W.; Ko, K. R.; Kim, H. K.; Lee, D. S.; Nam, I. J.; Lim, S.; Kim, S., Dehydrodiconiferyl Alcohol Inhibits Osteoclast Differentiation and Ovariectomy-Induced Bone Loss through Acting as an Estrogen Receptor Agonist. *J. Nat. Prod.* **2018,** 81, 1343-1356.
59. Lee, J.; Choi, J.; Kim, S., Effective suppression of pro-inflammatory molecules by DHCA via IKK-NF-kappaB pathway, in vitro and in vivo. *Br. J. Pharmacol.* **2015,** 172, 3353-3369.
60. Zhang, X.; Yu, Y.; Cen, Y.; Yang, D.; Qi, Z.; Hou, Z.; Han, S.; Cai, Z.; Liu, K., Bivariate Correlation Analysis of the Chemometric Profiles of Chinese Wild Salvia miltiorrhiza Based on UPLC-Qqq-MS and Antioxidant Activities. *Molecules* **2018,** 23, 538.
61. Villalva, M.; Jaime, L.; Aguado, E.; Nieto, J. A.; Reglero, G.; Santoyo, S., Anti-Inflammatory and Antioxidant Activities from the Basolateral Fraction of Caco-2 Cells Exposed to a Rosmarinic Acid Enriched Extract. *J. Agric. Food Chem.* **2018,** 66, 1167-1174.
62. Es-Safi, N.-E.; Kollmann, A.; Khlifi, S.; Ducrot, P.-H., Antioxidative effect of compounds isolated from Globularia alypum L. structure–activity relationship. *LWT - Food Sci Technol* **2007,** 40, 1246-1252.
63. Niu, H. S.; Hsu, F. L.; Liu, I. M., Role of sympathetic tone in the loss of syringin-induced plasma glucose lowering action in conscious Wistar rats. *Neurosci. Lett.* **2008,** 445, 113-116.